Lateral hypothalamus orexinergic inputs to lateral habenula modulate maladaptation after social defeat stress

Dan Wang [a],[1], Ao Li [a],[1], Keyi Dong [a],[1], Huihui Li [a], Yongxin Guo [a], Xinxin Zhang [a], Min Cai [b], Huiming Li [a], Guangchao Zhao [a],[**], Qianzi Yang [a],[*]

[a] *Department of Anesthesiology and Perioperative Medicine, Xijing Hospital, Xi'an, Shaanxi, China*
[b] *Department of Psychiatry, Xijing Hospital, Xi'an, Shaanxi, China*

ABSTRACT

Social stress, a common stressor, causes multiple forms of physical and mental dysfunction. Prolonged exposure to social stress is associated with a higher risk of psychological disorders, including anxiety disorders and major depressive disorder (MDD). The orexinergic system is involved in the regulation of multiple motivated behaviors. The current study examined the regulatory effect of orexinergic projections from the lateral hypothalamic area (LHA) to the lateral habenula (LHb) in depression- and anxiety-like behaviors after chronic social defeat stress. When mice were defeated during social interaction, both orexinergic neurons in the LHA and glutamatergic neurons in the LHb were strongly activated, as indicated by the FosTRAP strategy. Infusion of orexin in the LHb significantly alleviated social avoidance and depression-like behaviors induced by chronic social defeat stress. Administration of an orexin receptor 2 antagonist in the LHb further aggravated the depressive phenotype. Photoactivation of orexinergic cell bodies in the LHA or terminals in the LHb relieved anxiety-like behaviors induced by chronic social defeat stress. Collectively, we identified the antidepressant and anxiolytic effects of the circuit from LHA orexinergic neurons to the LHb in response to chronic social stress, providing new evidence of the antidepressant properties of LHA orexin circuits.

1. Introduction

Stress is the experience of physiological or psychological challenges, different valences of which lead to distinct responses (McEwen, 2007). Mild stress of a limited duration and intensity may lead to motivation and exhilaration, whereas prolonged stress, indicative of a continuously dangerous situation is associated with a higher risk of negative emotions, such as anxiety and depression (Kendler et al., 1999; McEwen, 2007). Social stress is one of the most common stressors in daily life, and studies have shown that cumulative social defeat stress is associated with an increased risk of anxiety disorders and major depressive disorder (MDD) (Barthas et al., 2020). In addition, social stress is also accompanied by multisystemic dysfunction, such as anorexia (Monteleone et al., 2020), hyperphagia (Razzoli et al., 2017), or insomnia (Van Someren, 2020), suggesting that complex brain networks are involved in regulating adaptations under social stress.

The animal model of social interaction between aggressive residents and defeated intruders provides a precise approach to investigate the response of stress receiver as well as the aggressive behavior (Golden et al., 2011; Kudryavtseva et al., 2014). Using such a social defeat model, Flanigan et al. recently reported that orexinergic projections from the lateral hypothalamic area (LHA) to the lateral habenula (LHb) encoded the aggressive behaviors of mice (Flanigan et al., 2020). However, whether this orexinergic innervation is responsible for the subsequent maladaptive behaviors in socially defeated mice, such as social avoidance, depression, and anxiety, remains unknown.

The orexinergic system has been implicated in the development and progression of depressive-like phenotypes (James et al., 2017) and responses to stress (Grafe and Bhatnagar, 2018). The orexin system consists of two peptides, orexin A (OA) and orexin B (OB), and two receptors, orexin receptor 1 (OxR1) and orexin receptor 2 (OxR2). The Orx2 receptor binds to OA and OB with similar high affinities, but Orx1

is more likely to bind to OA rather than OB (Ammoun et al., 2003). Orexinergic neurons are limited in the perifornical area of the lateral hypothalamus (PeF/LHA) and dorsomedial hypothalamus (Broberger et al., 1998; Nambu et al., 1999), but project widely to most brain regions (Sakurai, 2014). Preclinical studies have reported that both hypoactivity and hyperactivity of the orexinergic system could lead to depression in rodent models (Khairuddin et al., 2020). Mice treated with chronic mild stress (CMS) showed an increased percentage of Fos-positive orexinergic neurons in the PeF/LHA (Nollet et al., 2011). Multiple reports have also emphasized the regulatory role of OxR2 in depressive-like behaviors in animals (Arendt et al., 2014; Scott et al., 2011; Staton et al., 2018) and MDD in human trials (Brooks et al., 2019; De Boer et al., 2018; Recourt et al., 2019).

In addition, as the anti-reward center and a target of orexinergic projections in the brain, extensive studies have verified the critical role of the LHb in negative emotions and the pathophysiology of several psychiatric disorders, including depression (Hu et al., 2020). Exposure to chronic social stress significantly increases the excitability of LHb neurons (Huang et al., 2019). LHb neurons encode mRNA for both OxR1 and OxR2, but with higher proportion of OxR2 (Hashikawa et al., 2020). These studies suggest that orexinergic projections from the LHA to the LHb may also mediate depression-like behavior induced by social stress.

In the present study, we combined fiber photometry with optogenetics and neuropharmacology and observed the dynamic activity of orexinergic neurons in the LHA and glutamatergic neurons in the LHb in socially defeated mice. We also investigated the regulatory effect of orexinergic projections to the LHb on depression-like behaviors after social defeat stress.

2. Materials and methods

2.1. Animals

All experimental procedures were conducted according to the protocols approved by the Ethics Committee for Animal Experimentation and strictly adhered to the Guidelines for Animal Experimentation of the Fourth Military Medical University (Xi'an, China). All efforts were made to minimize animal suffering, to reduce the number of animals used, and to utilize alternatives to in vivo techniques, if available. For experimental wild-type animals, 10–12-week-old C57BL/6J male mice (25–30 g) and 5-month-old male CD-1 (ICR) mice (sexually experienced retired breeders) were purchased from Beijing Vital River Laboratory Animal Technology Co. Ltd. *Vglut2-ires-Cre* and *Gad2-ires-Cre* mice were provided by Jackson Laboratory (JAX Mice and Services), *Hcrt-Cre* mice were generously provided by Luis de Lecea (Stanford University, California, USA) and Zhian Hu (Third Military Medical University, Chongqing, China) (Giardino et al., 2018; Ren et al., 2018), and FosTRAP mice (*Fos-2A-iCreER*) were kindly provided by Peng Cao (National Institute of Biological Sciences, Beijing, China) (Shang et al., 2019). Mice were housed in home cages (3–5 animals per cage) before formal experiments began in a specific-pathogen-free environment with a constant temperature of 23 °C (22–24 °C) and humidity of 40% (38%–42%) on a 12/12-h light-dark cycle (lights on 07:00–19:00). All mice had *ad libitum* access to food and water, and only male mice were used in this study.

2.2. Virus construction

rAAV2/9-EF1a-DIO-mCherry or rAAV2/9-EF1a-DIO-ChR2-mCherry were used for optogenetic experiments, and rAAV2/9-EF1a-DIO-GCaMP6s or rAAV2/9-CAG-GCaMP6s were used for in vivo fiber photometry. All of the aforementioned viruses were provided by BrainVTA Technology Co., Ltd. (Wuhan, China).

2.3. Stereotaxic surgery

Mice were anesthetized in an induction chamber with 1.2% isoflurane (Baxter Healthcare, Puerto Rico) vaporized in oxygen at a flow rate of 1.0L/min and were then fixed to a stereotaxic frame while maintaining anesthesia with 0.8% isoflurane supplied through a mask. The skull was exposed and the viruses were then stereotactically injected into the LHA (AP: 1.80 mm, ML: 0.90 mm, DV: 5.10 mm) or LHb (AP: 1.72 mm, ML: 0.46 mm, DV: 2.65 mm) using Nanoject III (Drummond Scientific, Broomall, PA) at a slow rate of 23 nL/min via a micropipette. For drug treatments, all C57BL/6J male mice were placed on a stereotaxic apparatus, and a guide cannula (RWD, Inc., Shenzhen, China) was stereotaxically directed to the LHb. Mice were allowed to recover for at least 7 days after surgery.

2.4. Behavioral experiments

All behavioral experiments were video recorded. The behaviors were scored manually by a student who was blinded to the grouping or automatically measured using ANY-maze software (Stoelting Co., USA). Orexin-A (Tocris Bioscience, USA) were dissolved in saline at a concentration of 333 pmol/μL, and the OxR2 antagonist TCS-OX2-29 (Tocris Bioscience, USA) were dissolved in 5% DMSO to 33.3 μg/μL. The drugs were bilaterally injected into the LHb using a Hamilton syringe. The injection was controlled by a micro-pump (Pump 11plus, Harvard Apparatus, USA) at a speed of 0.04 μL/min for 5 min each side.

2.4.1. Social defeat stress

A modified paradigm of resident-intruder social interaction was used (Golden et al., 2011). The home cage of the CD1 mouse (resident) was divided longitudinally using perforated Plexiglas. A C57BL/6J mouse (intruder) was brought into the home cage of an aggressive CD1 mouse, but was separated by the perforated Plexiglas to allow for olfactory and minimal tactile contact. This phase lasted for 10 min. The intruder was then introduced into the resident's side of the cage and stayed together with the CD1 mouse for up to 5 min, or until five attacks on the intruder were observed. Once finished, the experimental C57BL/6J mouse was returned to the opposite side of the divider where it remained in visual and olfactory contact with the CD1 mouse for the next 24 h. During the following ten days, social defeat was established in the intruder mouse by repeating this procedure once per day.

The social interaction test was used to characterize the susceptibility of the defeated mice. Social avoidance/preference tests were performed in a square box (40 cm³) with a transparent perforated cylinder (diameter, 15 cm) set against the middle of one wall. Chronically defeated C57BL/6J mice were allowed to explore the box with the empty cylinder for 2.5 min, and then spent another 2.5 min exploring with an unfamiliar CD1 mouse placed in the cylinder. The social interaction ratio for the interaction zone was calculated by dividing the time in the interaction zone with the CD1 mouse present by the time in the absence of the CD1 mouse. Mice with a social interaction ratio <1 were categorized as susceptible. Only those with a significant social avoidance phenotype were used for further behavioral tests.

2.4.2. Tail suspension test (TST)

The tail suspension test was performed according to a previously reported method (Steru et al., 1985). Each mouse was suspended 60 cm above the floor upside-down by taping their tails. After the first 2 min of the test, the total duration of immobility (in seconds) was measured. An animal was considered immobile when it ceased moving its limbs and body, and only breathing movements were observed. After 6 min of tail suspension, the mice were placed back in their home cages.

2.4.3. Forced swimming test (FST)

The animal was placed in a glass cylinder (18 cm in height) filled with water (25 °C, 12 cm deep) for 4 min. After 1 min, the total duration

of immobility (in seconds) was measured. The mice were gently dried using a paper towel and placed back in their home cage after the test.

2.4.4. Open field test (OFT)

A plastic open field chamber (40 × 40 cm) was conceptually divided into a central field (20 × 20 cm) and a peripheral field for analysis. Each mouse was placed in the central field at the start of the test. The trajectory of each mouse was recorded using a camera placed above the open field. The apparatus was cleaned with 75% ethanol for each session. The number of times the mouse entered the central zone and amount of time spent in the central and peripheral areas were automatically analyzed using ANY-maze software.

2.4.5. Elevated plus maze (EPM) test

The elevated plus maze apparatus (Global Biotech Inc. Shanghai) was opaque and consisted of a central platform (10 cm × 10 cm), two open arms (50 cm × 10 cm), and two closed arms (50 cm × 10 cm) with 40-cm high protective walls, 70 cm above the ground. Animals were placed on the central platform facing one of the open arms and were free to explore the maze for 5 min. The apparatus was cleaned with 75% ethanol before and after each session. Traces were recorded using an overhead camera and were shown as a track plot for each group. The proportion of time spent exploring the open arms was calculated.

2.5. Fiber photometry

Mice were implanted with an optical fiber (diameter: 200 μm, NA: 0.37, Inper, Hangzhou, China) into the LHA or LHb after virus injection. After surgery, mice were housed individually to enable full recovery. For the fiber photometry experiments, the implanted fiber was attached to an optical photometer (ThinkerTech, Nanjing, China). A 488-nm continuous LED light beam was emitted and reflected by a dichromic mirror, and the GCaMP6s fluorescence was focused and recorded using a photometer. To reduce the bleaching of GCaMP, the laser intensity at the fiber tip was regulated to 30–40 μW. The average $\Delta F/F$ (%) values shown in bar graphs were calculated as $(F_{duration} - F_{baseline})/F_{baseline} \times 100$, where $F_{baseline}$ is the mean GCaMP signal for the window before the time zero. Stimuli were given in short sequences, and the GCaMP signal was recorded 3 s before and after being defeated. For Z-score normalization, the formula for the Z-score was $(D - μ)/σ$, where D is the raw fiber photometry signal data, μ is the mean value of the raw data, and σ is the standard deviation of the raw data. The Z-score data were divided into two 2-s sections by time zero.

2.6. Optogenetic experiments

For optogenetic experiments, a fiber patch cord was connected to the laser generator, and the optic fibers were connected to the fiber patch through a rotary joint (ThinkerTech, Nanjing, China). Optical activation was performed using a 473-nm laser (20Hz, 20 ms, 10 μW). All stimulations were given during behavioral tests.

2.7. Immunohistochemistry

Mice were deeply anesthetized with isoflurane and transcardially perfused with 4% paraformaldehyde followed by 0.9% saline. Brains were postfixed for 2 h in 4% paraformaldehyde at 4 °C and were then serially transferred to 30% sucrose in phosphate-buffered saline (PBS, PH = 7.4). The brains were coronally sectioned every 40 μm using a Leica cryostat. The sectioned brains were washed with PBS for 5 min three times consecutively, and blocked with 5% normal donkey serum in PBS with Triton X-100 for 2 h at 24–26 °C. Primary antibodies, including rabbit anti-glutamate (1:1000, Sigma-Aldrich), mouse anti-orexin A (1:200, Santa Cruz), mouse anti-OxR2 (1:200, GeneTex), rabbit anti-c-Fos (1:1000, Sigma-Aldrich) and rabbit anti-GABA (1:200, GeneTex) were incubated at 4 °C overnight. The slices were washed with PBS. The

incubation of secondary antibodies, including donkey anti-rabbit Alexa Fluor 488 (1:400, Jackson ImmunoResearch), donkey anti-mouse Alexa Fluor 488 (1:400, Jackson ImmunoResearch), donkey anti-rabbit Cy3 (1:400, Jackson ImmunoResearch) or donkey anti-mouse Cy3 (1:400, Jackson ImmunoResearch), were then incubated for 2 h at 24–26 °C. The brain slices were washed with PBS again after incubation, and sections were mounted in Fluoromount-G (Millipore) and imaged using a confocal microscope (FV1200, Olympus).

2.8. 2.8. statistical analysis

All statistical analyses were performed using MATLAB R2018b (MathWorks) or Prism 8.0.1 (GraphPad) software. No statistical methods were used to predetermine sample sizes, however, our sample sizes were similar to those reported in previous publications. Individual data points are shown in all of the relevant figures. The *n* values used for these analyses represent the number of mice or cells in each group. All data are presented as the mean ± standard error of mean (SEM) unless otherwise stated in the figure legends. Two-sided Student's *t*-test or one-way analysis of variance (ANOVA) followed by Bonferroni tests were used for statistical analyses of experimental data. P-values < 0.05 were considered to indicate statistical significance.

3. Results

3.1. The LHA^{Orx}-LHb^{Glu} circuit is activated by social stress

To investigate the specific brain regions activated by negative social stimuli, we employed a FosTRAP strategy described previously to genetically label neurons activated under social stress conditions (Allen et al., 2017; Shang et al., 2019). By crossing the transgenic mouse line expressing CreER under the control of the *Fos* promoter (Fos-2A-iCreER) with a Cre-dependent tdTomato (tdT) reporter mouse line (RosaTD), we were able to temporally control the expression of tdT in Fos-positive neurons with the application of 4-hydroxytamoxifen (4-OHT) (Fig. 1a). The Fos-2A-iCreER:RosaTD mice were treated with 4-OHT and then were attacked by an aggressive male CD1 mouse for 1 min each time; this was repeated four times consecutively with 14-min intervals (Fig. 1a). This procedure resulted in a significant increase in tdT expression in both the LHA and LHb in defeated mice, suggesting that the neurons in these two nuclei were activated (Fig. 1b and c).

To examine the subtype of social stress-activated neurons in the LHA and LHb, we co-stained the Fos with glutamate or GAD2 in the LHb or with orexin A peptide in the LHA. We found that acute social stress boosted the proportion of Fos-positive glutamatergic neurons from 4.896 ± 0.3217% to 75.25 ± 1.751% in the LHb. In contrast, the proportion of Fos-labeled LHb GABAergic neurons slightly decreased after social stress (59.32 ± 1.829% vs. 47.99 ± 2.241%, p = 0.0012) (Fig. 1d and e). In the LHA, 76.05 ± 1.905% of orexinergic neurons were Fos-positive (Fig. 1f and g). To further confirm the involvement of projections from LHA orexinergic (LHA^{Orx}) neurons to LHb glutamatergic neurons (LHb^{Glu}) in the neural response to social defeat, we assessed the co-localization of orexin receptor 2 (OxR2) (Li et al., 2019) with Fos-positive neurons and glutamatergic neurons in the LHb, respectively. The proportion of Fos-positive OxR2-expressing neurons increased from 28.50 ± 0.8929% to 79.76 ± 2.069% after acute social stress in the LHb (Fig. 1d), while normally 49.74 ± 2.970% of LHb OxR2-expressing neurons were glutamatergic (Fig. 1h). We also confirmed the activation of LHA orexinergic neurons (25.94 ± 3.438% vs. 76.49 ± 3.994%, p < 0.0001) (Supplementary Figs. 1a and b) and LHb glutamatergic neurons (12.27 ± 1.129% vs. 68.77 ± 2.573%, p < 0.0001) (Supplementary Figs. 1c and d) after 10 consecutive days of social stress, which was not significantly different from the acute stress activation. These results collectively suggest that LHA^{Orx} neurons, LHb^{Glu} neurons and their projections could participate in the internal response to social defeat stress.
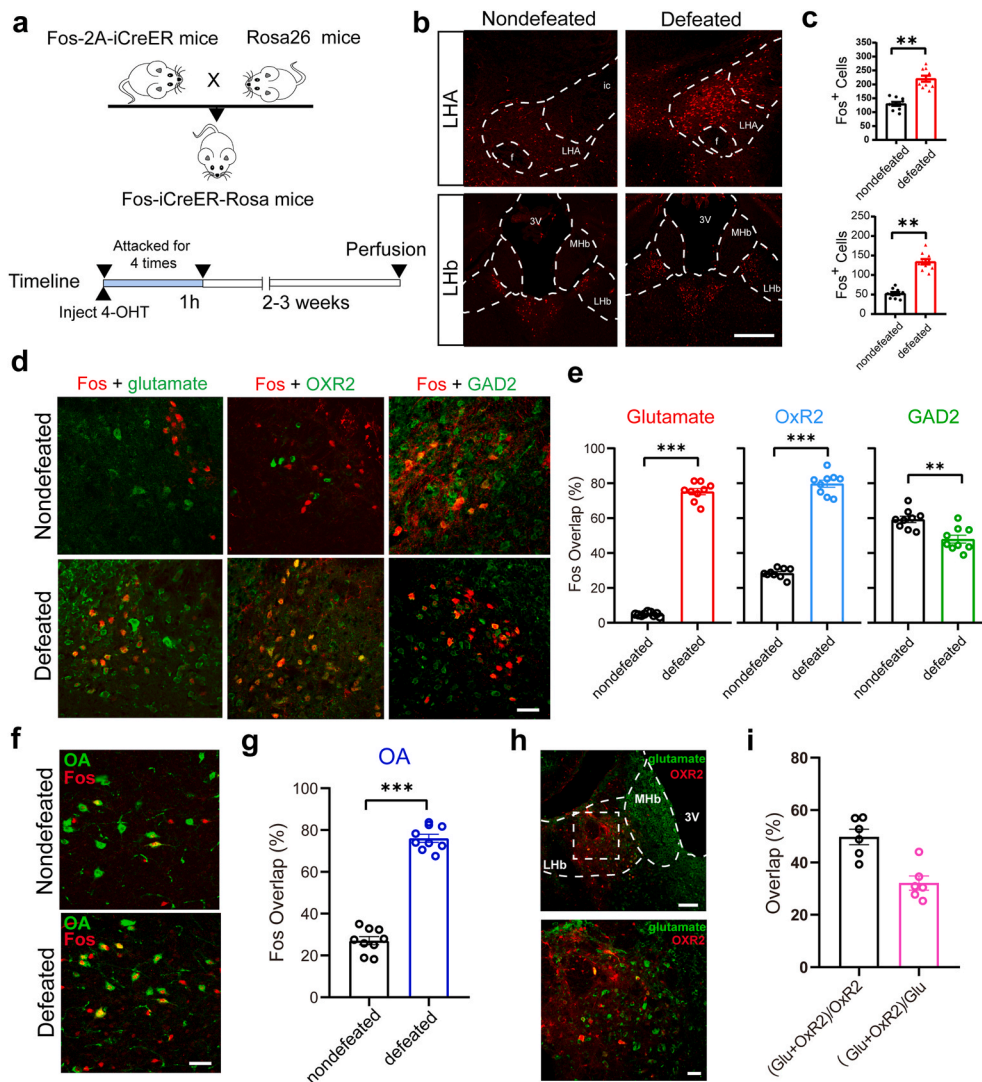
Fig. 1. Activation of the LHA^{Orx}-LHb^{Glu} circuit after social defeat stress
(**a**) Experimental design of the FosTRAP strategy. (**b**) Representative tdTomato expression in the LHA (top) and LHb (bottom) of nondefeated and defeated mice. (**c**) Quantification of Fos-positive cells in the LHA (top, 129.9 ± 6.877 vs. 220.4 ± 10.77, t = 7.080, p < 0.0001) and LHb (bottom, 52.40 ± 3.879 vs. 134.1 ± 6.993, t = 10.22, p < 0.0001) of non-defeated and defeated mice. (**d**) Representative overlap of tdTomato expression with neurons expressing glutamate (left), OxR2 (middle), and GAD2 (right) in the LHb of non-defeated (top) and defeated (bottom) mice. (**e**) Percentage of Fos-positive neurons in neurons expressing glutamate (left, 4.896 ± 0.3217% vs. 75.25 ± 1.751%, t = 39.52, p < 0.0001), OxR2 (middle, 28.50 ± 0.8929% vs. 79.76 ± 2.069%, t = 22.75, p < 0.0001), and GAD2 (right, 59.32 ± 1.829% vs. 47.99 ± 2.241%, t = 3.917, p = 0.0012) in non-defeated and defeated mice. (**f**) Representative overlap of tdTomato expression with the neurons expressing orexin A (OA) in the LHA of non-defeated (top) and defeated (bottom) mice. (**g**) Percentage of Fos-positive neurons in the OA-expressing neurons (27.07 ± 1.968% vs. 76.05 ± 1.905%, t = 17.88, p < 0.0001) of nondefeated and defeated mice. (**h**) Representative overlap of the neurons expressing glutamate and OxR2 in the LHb. (**i**) Percentage of glutamate expression among OxR2-positive neurons (49.74 ± 2.970%) and OxR2 expression among glutamate positive neurons (32.15 ± 2.689%). Data are presented as mean ± standard error of the mean. *p < 0.05, **p < 0.01, and ***p < 0.001 (unpaired t-test). LHA, lateral hypothalamic area; LHb, lateral habenula.

3.2. Neuronal activity of the LHA^{Orx}-LHb^{Glu} circuit is closely related to social defeat behavior

To further investigate how the LHA and LHb respond to social defeat stress in vivo, we injected the AAV virus expressing GCaMP6 into the LHA and LHb to temporally measure the transient calcium activity during social interactions (Fig. 2a–c, Supplementary Figs. 2a and b). In wild-type mice, we found that the overall activity of the LHb was promptly elevated while the mice were being attacked (Supplementary Figs. 2c–e). We then separately recorded the neuronal activities of LHb^{Glu} neurons in Vglut2-cre mice and LHA^{Orx} neurons in Hcrt-cre mice during social interactions. Both LHb^{Glu} neurons and LHA^{Orx} neurons showed a robust increase in calcium signaling in defeated mice during each attack (Fig. 2d–i). However, GABAergic neurons in the LHb did not show such an increase in neuronal activity (Supplementary Figs. 2f–h), indicating a close relationship between the activation of the LHA^{Orx}-LHb^{Glu} circuit with social defeat behavior.

3.3. Enhancement of orexin signaling in the LHb alleviates depression-like behavior induced by social defeat stress

To assess the regulatory effect of the orexinergic projections to the LHb on depression-like behavior induced by chronic social defeat stress (CSDS), we administered orexin A (OA) into the LHb in wild-type

stressed mice (Fig. 3a). After completing a 10-day CSDS procedure, mice displayed distinct adaptive behaviors after the social interaction test. Mice susceptible to CSDS spent less time in the interaction zone and more time in the corner zone than those resilient to CSDS when CD1 mice were placed in the cylinder (Fig. 3b–d). Mice susceptible to CSDS were selected for further studies. Bilateral microinjection of OA into the LHb significantly alleviated social avoidance behaviors, as indicated by the increased social interaction (SI) ratio for the interaction zone (0.5292 ± 0.1073 vs. 1.137 ± 0.1453, p = 0.0046) and the decreased SI ratio for the corner zone (3.990 ± 0.8926 vs. 0.7431 ± 0.2286, p = 0.0034) in the social interaction test (Fig. 3e–g). In addition, without affecting the total travel distance and travel distance in the interaction zone, enhancement of orexin signaling reduced the travel distance in the corner zone (Fig. 3i–k). Furthermore, depression-like behaviors induced by CSDS were improved by OA microinjection, as the immobility time was shortened by 10.10% (57.86 ± 1.817% vs. 47.76 ± 3.137%, p = 0.0145) in the tail suspension test and 8.84% (29.37 ± 2.714% vs. 20.53 ± 1.472%, p = 0.0125) in the forced swimming test (Fig. 3l, m). Similar experiments were performed following microinjection of the OxR2 antagonist, TCS-OX2-29 (Supplementary Figs. 3a–d). In contrast, TCS-OX2-29 further exacerbated social avoidance behavior as mice spent more time in the corner of the test cage (Fig. 4a and b). Although OxR2 antagonism reduced the total distance traveled in the social interaction test (7.827 ± 0.8908 m vs. 4.840 ± 0.7645 m, p = 0.0234), the travel
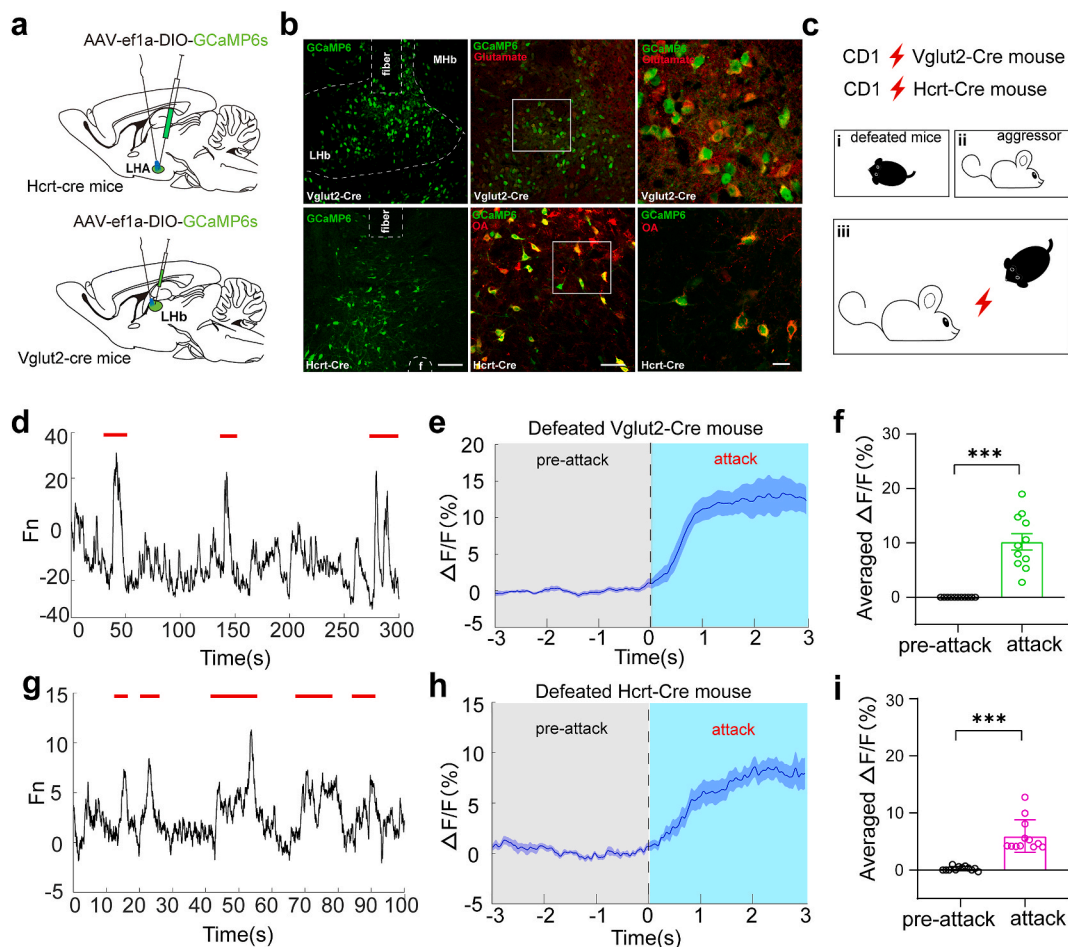
Fig. 2. Increment of neuronal calcium signals in LHA orexinergic neurons and LHb glutamatergic neurons during social defeat stress
(**a**) Schematic diagram of virus injection and fiber implantation. (**b**) Verification of virus expression in LHb glutamatergic neurons (top) and LHA orexinergic neurons (bottom). (**c**) Experimental design of *in-vivo* calcium imaging during social interactions. (**d**) Representative calcium activities in LHb glutamatergic neurons during attacks (indicated by short red lines). (**e**) Calcium activities in glutamatergic neurons in the LHb before and after attacks (the mean and SEM are represented by the full line and shaded area, respectively). (**f**) Average $\Delta F/F$ before and after attacks ($-0.001542 \pm 0.001077\%$ vs. $10.19 \pm 1.499\%$, t $= 6.795$, p < 0.0001). (**g**) Representative calcium activities in LHA orexinergic neurons during attacks (indicated by the short red lines). (**h**) Calcium activities in orexinergic neurons in the LHA before and after attacks (the mean and SEM are represented by the full line and shaded area). (**i**) Average $\Delta F/F$ before and after attacks ($0.2515 \pm 0.1031\%$ vs. $5.925 \pm 0.8203\%$, t $= 7.518$, p < 0.0001). Data are presented as mean $\pm$ SEM. ***p < 0.001 (unpaired *t*-test). LHA, lateral hypothalamic area; LHb, lateral habenula. . (For interpretation of the references to colour in this figure legend, the reader is referred to the Web version of this article.)

distances in the interaction zone (1.414 ± 0.1901 m vs. 1.136 ± 0.1188 m, p $= 0.2361$) and corner zone (1.143 ± 0.1699 m vs. 0.9391 ± 0.1808 m, p $= 0.4245$) were unaffected (Fig. 4c–e). TCS-OX2-29 also significantly prolonged immobilization when mice were tail-suspended ($52.86 \pm 1.988\%$ vs. $60.31 \pm 1.356\%$, p $= 0.0079$) or forced to swim ($24.71 \pm 1.967\%$ vs. $33.91 \pm 1.362\%$, p $= 0.0038$) (Fig. 4f and g), suggesting that OxR2 could mediate the anti-depressive effect of the LHA^{Orx}-LHb^{Glu} circuit.

3.4. Optogenetic activation of the LHA^{Orx}-LHb^{Glu} circuit rescues the maladaptive behaviors after social defeat stress

Apart from depression, chronic stress also leads to behavioral maladaptation, such as anxiety. To further determine whether the LHA^{Orx}-LHb^{Glu} circuit plays a role in the modulation of anxiety-like behaviors induced by chronic social stress, we combined optogenetics and the elevated plus maze (EPM) or open field test (OFT). We injected AAV-Ef1a-DIO-ChR2-mCherry virus into the LHA of Hcrt-cre mice to express light-sensitive channelrhodopsin in LHA^{Orx} neurons (Fig. 5a and b). By applying blue light through the optical fiber, we found that optical activation of LHA^{Orx} cell bodies or orexinergic projection terminals in

the LHb increased the time spent in the open arms (cell bodies, 16.41 ± 2.084 s vs. 120.8 ± 23.04 s, p $= 0.0007$; projection terminals, 20.19 ± 3.270 s vs. 71.49 ± 11.53 s, p $= 0.0011$) and entries into the open arms (cell bodies, 3.286 ± 0.7781 vs. 8.714 ± 1.809, p $= 0.0174$; projection terminals, 3.429 ± 0.7190 vs. 14.14 ± 2.444, p $= 0.0012$) of the EPM (Fig. 5c–j). Photostimulation of both LHA^{Orx} cell bodies and projections to the LHb also reduced the time spent in the closed arms (cell bodies, 232.0 ± 8.361 s vs. 113.7 ± 22.63 s, p $= 0.0002$; projection terminals, 234.7 ± 7.556 s vs. 187.9 ± 14.60 s, p $= 0.0128$) (Fig. 5e, i). In the OFT, optical activation of LHA^{Orx} cell bodies or LHb terminals increased the time mice stayed in the central area (cell bodies, 12.34 ± 0.7521 s vs. 21.97 ± 2.647 s, p $= 0.0108$; projection terminals, 12.70 ± 0.8678 s vs. 23.60 ± 1.438s, p $= 0.0002$), the number of times the mice crossed the line dividing the central and peripheral areas (cell bodies, 48.60 ± 5.810 vs. 100.5 ± 13.33, p $= 0.0090$; projection terminals, 49.80 ± 4.420 vs. 104.5 ± 9.451, p $= 0.0009$), and the total mobile time (cell bodies, 69.90 ± 4.800 s vs. 113.4 ± 10.23 s, p $= 0.0058$; projection terminals, 72.20 ± 5.798 s vs. 131.9 ± 9.382 s, p $= 0.0006$) (Fig. 5k-r). Together, these data suggest that activation of the LHA^{Orx}-LHb^{Glu} circuit could efficiently improve anxiety-like behaviors induced by CSDS.
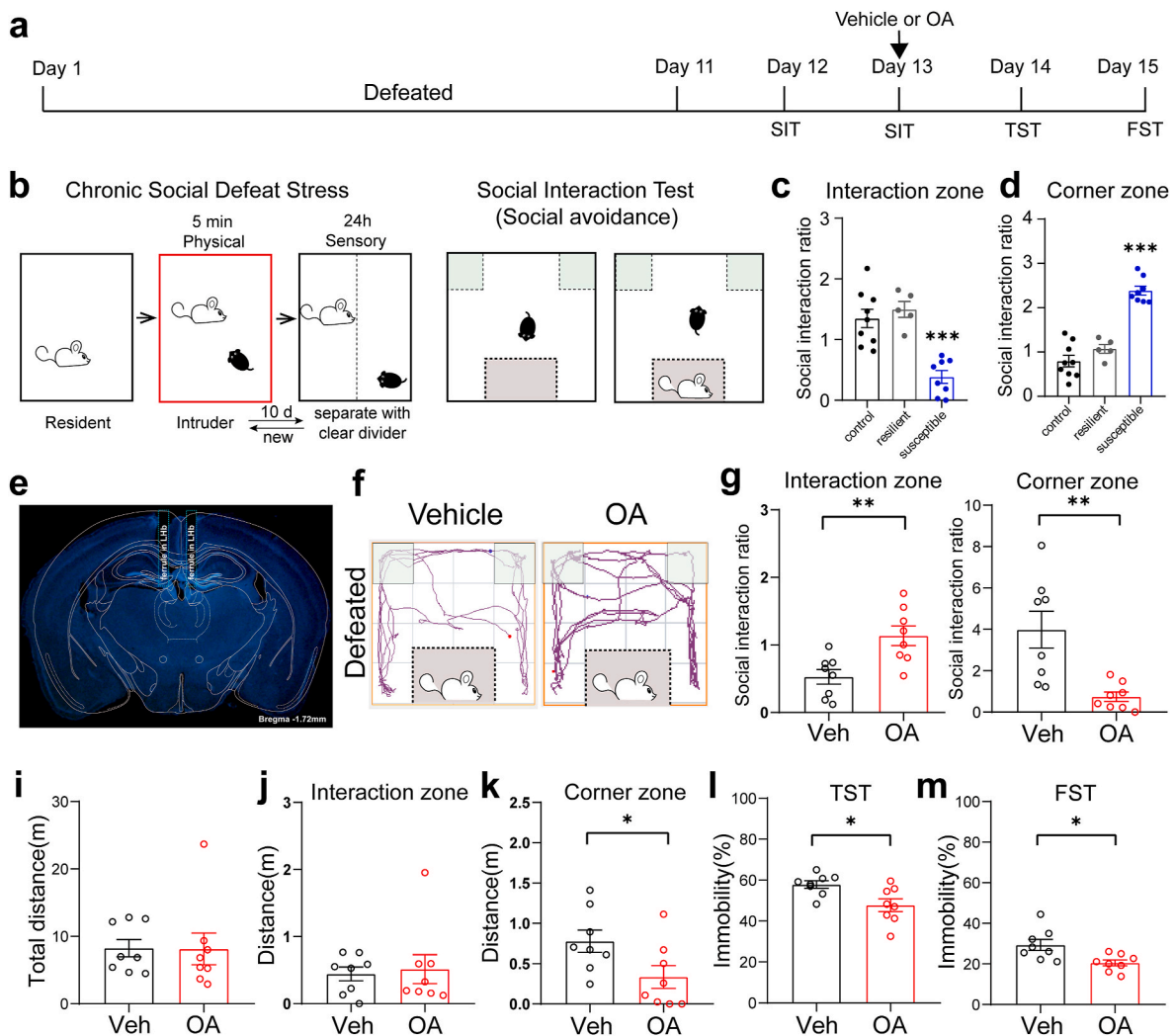
Fig. 3. Infusion of orexin A (OA) into the LHb alleviated social avoidance and depressive behaviors after chronic social defeat stress
(**a**) The experimental protocol for chronic social defeat stress (CSDS), as well as the timing of pharmaceutical administration, the social interaction test (SIT), tail suspension test (TST), and forced swimming test (FST). (**b**) Schematic procedure of CSDS modeling (left) and the social interaction test (right). Intruder mice were divided into the susceptible and resilient groups using the social interaction test. Mice who were susceptible to CSDS had a lower social interaction ratio in the interaction zone (**c**) but higher ratio in the corner zone (**d**) when the CD1 mouse was present (one-way ANOVA with Bonferroni's post hoc comparisons, F = 19.32 and F = 55.30, respectively, p < 0.001 for both). (**e**) Representative image of the location of the microinjection canula. (**f**) Representative trajectories in the SIT of susceptible mice with infusion of vehicle (left) or OA (right) into the LHb. (**g**) Infusing OA into the LHb increased the social interaction ratio in the interaction zone (left, 0.5292 ± 0.1073 vs. 1.137 ± 0.1453, t = 3.364, p = 0.0046) and reduced the social interaction ratio in the corner zone (right, 3.990 ± 0.8926 vs. 0.7431 ± 0.2286, t = 3.524, p = 0.0034). Infusing OA into the LHb did not affect the (**i**) total travel distance (8.251 ± 1.295m vs. 8.145 ± 2.346m, t = 0.03942, p = 0.9691) or (**j**) the travel distance in the interaction zone (0.4438 ± 0.1022m vs. 0.5156 ± 0.2161m, t = 0.3006, p = 0.7681), but decreased the (**k**) travel distance in the corner zone (0.7790 ± 0.1378m vs. 0.3356 ± 0.1416m, t = 2.244, p = 0.0415). (**l**) Infusion of OA into the LHb reduced the percentage of immobility time in the TST ($57.86 \pm 1.817\%$ vs. $47.76 \pm 3.137\%$, t = 2.787, p = 0.0145), and the (**m**) percentage of time spent immobile in the FST ($29.37 \pm 2.714\%$ vs. $20.53 \pm 1.472\%$, t = 2.865, p = 0.0125). Data are presented as the mean ± SEM *p < 0.05, **p < 0.01, ***p < 0.001 (unpaired *t*-test). LHb, lateral habenula.

4. Discussion

In the present study, we utilized multidisciplinary methods to investigate the regulatory role of the LHA^Orx-LHb^Glu circuit in depression and anxiety-like behaviors after social defeat stress in mice. The FosTRAP strategy revealed a strong correlation between social defeat stress and the activation of orexinergic neurons in the LHA and glutamatergic neurons in the LHb. A large population of OxR2-expressing neurons in the LHb was found to be glutamatergic, and a number of Fos-positive neurons induced by social defeat expressed OxR2, which provides evidence for the involvement of the LHA^Orx-LHb^Glu circuit in the intrinsic response to social stress. Pharmacological activation of orexinergic signaling in the LHb effectively alleviated CSDS-induced social avoidance and reduced immobilization in the FST and TST. This

antidepressant effect was partially dependent on the effect of OxR2 on glutamatergic neurons in the LHb. Additionally, opto-activation of LHA orexinergic neurons or LHb glutamatergic neurons also considerably relieved anxiety-like behaviors after social defeat.

Orexins are known to mediate stress-induced responses. Acute stressors such as forced swim stress or restraint stress increased Fos expression in orexinergic neurons and orexin A levels in the cerebrospinal fluid (Chang et al., 2007; Grafe, Eacret, et al., 2017). Restraint stress also robustly excited orexinergic neurons by improving calcium signals in a fiber photometry study (Gonzalez et al., 2016). Orexins could then activate the sympathetic nervous system and promote the hypothalamic-pituitary-adrenal (HPA) axis response to acute stress as indicated by increased levels of corticotropin-releasing hormone (CRH), adrenocorticotropic hormone (ACTH) and corticosterone (Grafe and
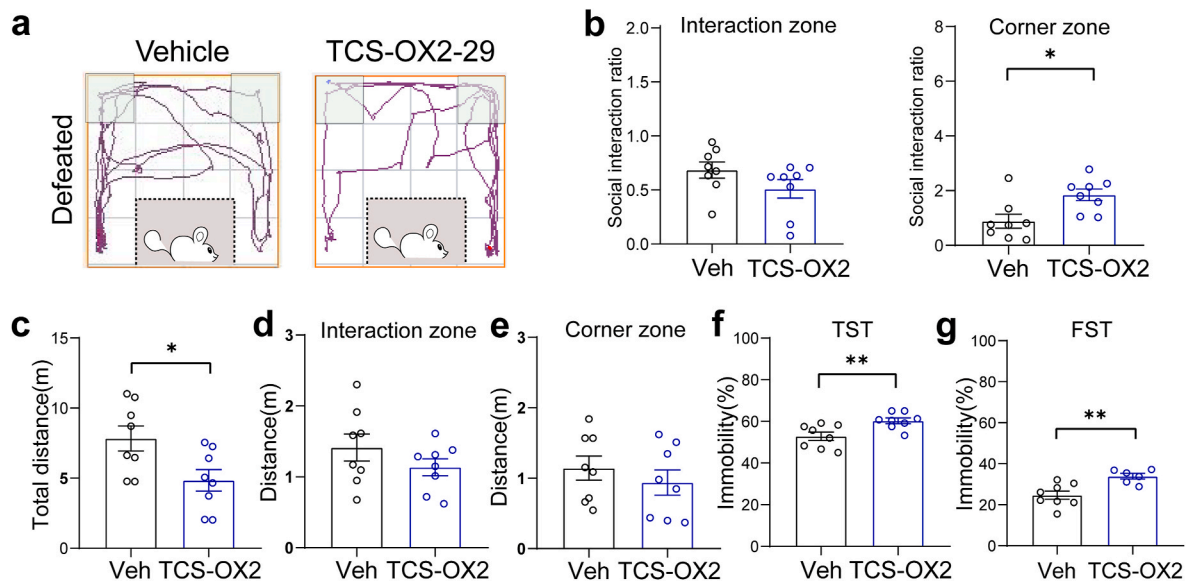
Fig. 4. Infusion of OxR2 antagonist into the LHb exacerbated social avoidance and depressive behaviors after chronic social defeat stress

(**a**) Representative trajectories in the social interaction tests of susceptible mice with administration of vehicle (left) or TCS-OX2-29 (right) into the LHb. (**b**) Infusion of TCS-OX2-29 into the LHb did not affect the social interaction ratios in the interaction zone (left, 0.6843 ± 0.07429 vs. 0.5095 ± 0.08592, t = 1.538, p = 0.1463) but increased the ratio in the corner zone (right, 0.8814 ± 0.2580 vs. 1.844 ± 0.2147, t = 2.869, p = 0.0124). Infusion of TCS-OX2-29 reduced the (**c**) total travel distance in the social interaction test (7.827 ± 0.8908m vs. 4.840 ± 0.7645m, t = 2.545, p = 0.0234), but did not increase (**d**) travel distance in the interaction zone (1.414 ± 0.1901m vs. 1.136 ± 0.1188m, t = 1.238, p = 0.2361) or (**e**) corner zone (1.143 ± 0.1699m vs. 0.9391 ± 0.1808m, t = 0.8227, p = 0.4245). Infusion of TCS-OX2-29 increased the (**f**) percentage of time spent immobile in the tail suspension test (52.86 ± 1.988% vs. 60.31 ± 1.356%, t = 3.095, p = 0.0079) and (**g**) percentage of time spent immobile in the forced swimming test (24.71 ± 1.967% vs. 33.91 ± 1.362%, t = 3.577, p = 0.0038). Data are presented as the mean ± SEM. *p < 0.05, **p < 0.01 (unpaired *t*-test). LHb, lateral habenula.

Bhatnagar, 2018). In the current study, we demonstrated that acute social stress promptly activated the LHA orexinergic neurons and LHb glutamatergic neurons by increasing the expression of Fos and elevating the transient calcium signals. This provides evidence for the involvement of orexins and LHb in the prompt response of socially defeated mice. Of note, after 10 days of repeated stress, orexinergic neurons and LHb glutamatergic neurons still showed a significant increase in c-Fos expression in response to the last round of social defeat stress in the susceptible mice. Therefore, it is reasonable to postulate that the repeated activation of orexinergic neurons and their projections to the LHb could contribute to the maladaptive behaviors related to CSDS.

Surprisingly, we found that the enhancement of orexinergic signaling using the optogenetic approach or administration of OA in the LHb reversed the depression or anxiety-like behaviors after CSDS, whereas infusion of the OxR2 antagonist in the LHb exacerbated these depression-like behaviors, suggesting an anti-depressive and anxiolytic role of the orexinergic projections from the LHA to the LHb. In line with our findings, several previous studies have showed that intra-cerebroventricular administration of orexin A significantly reduced the immobility time in the FST (Ito et al., 2008), and increased time spent in the open arms of EPM, indicating reduced anxiety behaviors after chronic exposure to predator-scent stress (Cohen et al., 2020). In addition, activation of orexinergic neurons via calorie restriction after the social defeat was also reported to elicit an antidepressant effect as indicated by prolonged latency to immobility and shortened immobility duration in the FST (Lutter et al., 2008). In contrast, Grafe et al. found that reduced orexin levels were correlated with resilience to repeated social defeat stress. However, they also found that chemogenetic inhibition of orexinergic neurons increased depressive-like behavior in non-stressed animals (Eacret et al., 2019; Grafe et al., 2018), indicating that the anti-depressive effect of orexins likely depends on the brain states (Chung et al., 2014). In fact, both the reduction (Blouin et al., 2013; Brundin, Björkqvist, et al., 2007; Brundin, Petersén, et al., 2007; Lutter et al., 2008; Nocjar et al., 2012) and the increment (Arendt et al., 2013; Jalewa et al., 2014; Mikrouli et al., 2011; Nollet et al., 2011) of

orexin levels were found to be related to depression behaviors in pre-clinical and clinical studies. Together, these paradoxical evidences together raise the possibility that diverse brain states may preferentially activate certain orexin circuits, which leads to the distinct regulatory functions of orexin on depressive behaviors. Recent studies have reported that orexin could excite GABAergic neurons in the ventral pallidum (VP) to promote social stress resilience and prevent depression-like behaviors (Ji et al., 2019), and that microinjection of orexin A into the central amygdala induces anxiolytic effects (Pan et al., 2020). Conversely, suppression of orexin signaling in the basolateral amygdala has been suggested to exert an antidepressant effect (Kim et al., 2015). The distinct natures of these targeting nuclei are likely partially responsible for the different roles of orexins. The LHb is known for its negative regulation of various reward circuitries and the primary function of encoding aversive states (Hu et al., 2020). Fos staining and calcium imaging results in our study showed that social defeat stress also induced the activation of LHb neurons, which was consistent with previous studies on the nature of the LHb in response to various stressors (Wang et al., 2017). The burst firing patterns of LHb glutamatergic neurons are closely related to the depressive behaviors (Cui et al., 2018; Yang et al., 2018). Exposure to CSDS significantly increased the excitability and burst firing in the LHb, and inhibition of LHb neurons alleviated the depression-like behaviors tested in social interaction tests, as well as anxiety-like behaviors in EPM tests (Huang et al., 2019). Therefore, it is possible that orexinergic innervation in the LHb could elicit an antidepressant effect by regulating the burst firing of LHb neurons; however, this needs further investigation.

In addition, orexins bind to two different G protein-coupled receptors, OxR1 and OxR2 (Sakurai, 2014), which appear to have opposite regulatory effects on depression and anxiety (Summers et al., 2020). OxR1 knockout and OxR1 antagonism resulted in reduced immobility durations in FST and TST (Scott et al., 2011), and OxR1 gene variants are associated with the risk and development of MDD in clinical patients (Cengiz et al., 2019; Rainero et al., 2011). In contrast, knockdown of BLA OxR2 aggravates the anxiety-like behaviors induced by chronic
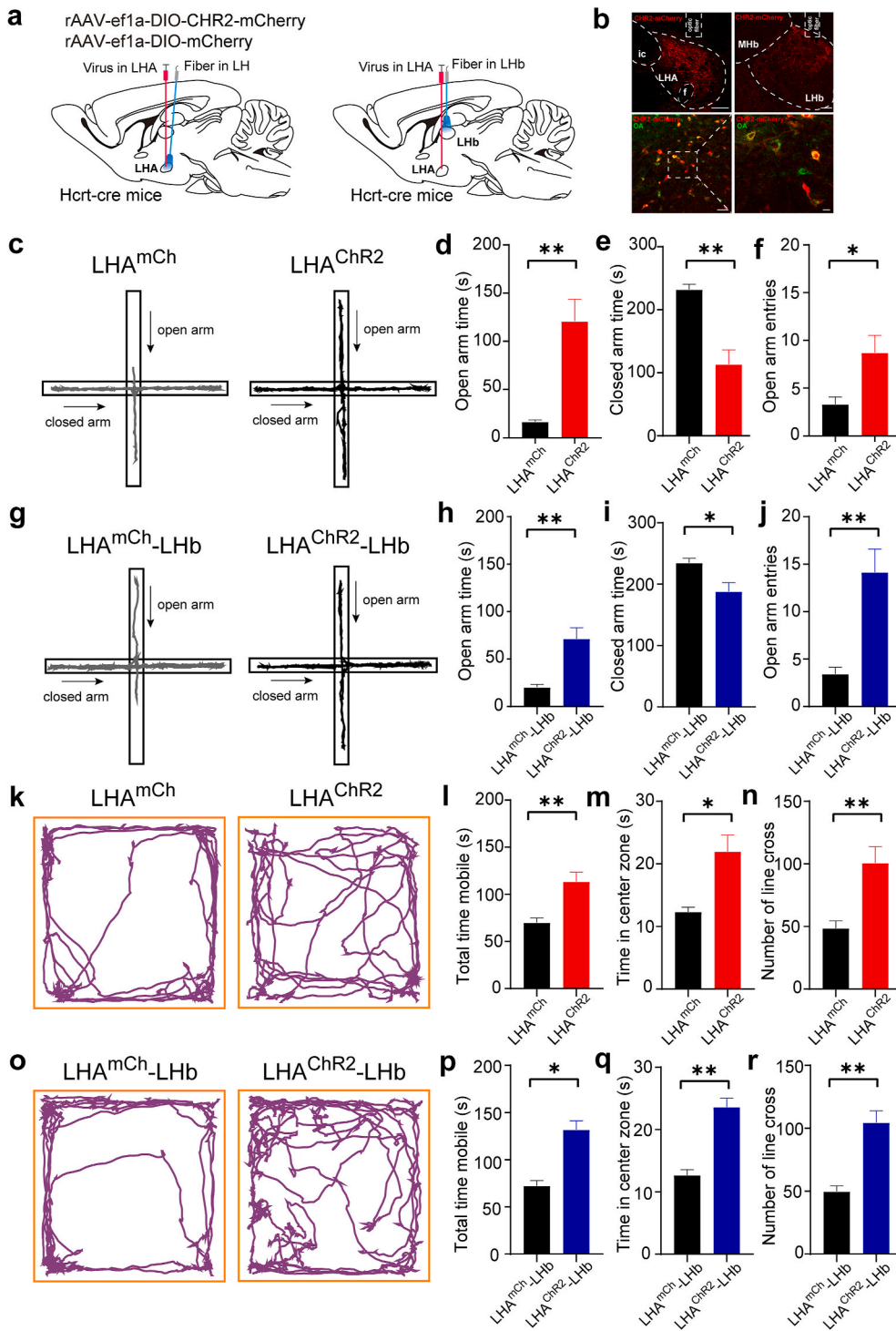
Fig. 5. Optogenetic activation of the LHA^{Orx}-LHb^{Glu} circuit relieved anxiety-like behaviors after chronic social defeat stress (**a**) Schematic diagram of virus injection and fiber implantation into the LHA (LHA^{mCh} represents the mCherry control group and LHA^{ChR2} represents the optogenetic activation group) or the LHb (LHA^{mCh}-LHb represents the control group and LHA^{ChR2}-LHb represents the optogenetic activation group) of the Hcrt-cre mice. (**b**) Representative images of virus expression and optical fiber placement. (**c**) Representative trajectories of LHA^{mCh} and LHA^{ChR2} mice in the elevated plus maze test. (**d**) Time spent in the open arms during optogenetic activation of LHA^{mCh} and LHA^{ChR2} (16.41 ± 2.084 s vs. 120.8 ± 23.04 s, t = 4.511, p = 0.0007). (**e**) Time spent in the closed arms with optogenetic activation of LHA^{mCh} and LHA^{ChR2} (232.0 ± 8.361 s vs. 113.7 ± 22.63 s, t = 4.906, p = 0.0002). (**f**) Number of entries into the open arms during optogenetic activation of LHA^{mCh} and LHA^{ChR2} (3.286 ± 0.7781 vs. 8.714 ± 1.809, t = 2,757, p = 0.0174). (**g**) Representative trajectories of LHA^{mCh}-LHb and LHA^{ChR2}-LHb mice in the elevated plus maze test. (**h**) Time spent in the open arms with optogenetic activation of LHA^{mCh}-LHb and LHA^{ChR2}-LHb (20.19 ± 3.270 s vs. 71.49 ± 11.53 s, t = 4.280, p = 0.0011). (**i**) Time spent in the closed arms during optogenetic activation of LHA^{mCh}-LHb and LHA^{ChR2}-LHb (234.7 ± 7.556 s vs. 187.9 ± 14.60 s, t = 2.850, p = 0.0128). (**j**) Number of entries into the open arms during optogenetic activation of LHA^{mCh}-LHb and LHA^{ChR2}-LHb (3.429 ± 0.7190 vs. 14.14 ± 2.444, t = 4.206, p = 0.0012). (**k**) Representative trajectories of LHA^{mCh} and LHA^{ChR2} mice in the open field test. (**l**) Total mobile time in the open field during optogenetic activation of LHA^{mCh} and LHA^{ChR2} (69.90 ± 4.800 s vs. 113.4 ± 10.23 s, t = 3.592, p = 0.0058). (**m**) Time spent in the center zone of the open field during optogenetic activation of LHA^{mCh} and LHA^{ChR2} (12.34 ± 0.7521 s vs. 21.97 ± 2.647 s, t = 3.204, p = 0.0108). (**n**) Number of line crossings in the open field during optogenetic activation of LHA^{mCh} and LHA^{ChR2} (48.60 ± 5.810 vs. 100.5 ± 13.33, t = 3.319, p = 0.0090). (**o**) Representative trajectories of LHA^{mCh}-LHb and LHA^{ChR2}-LHb mice in the open field test. (**p**) Total mobile time in the open field during optogenetic activation of LHA^{mCh}-LHb and LHA^{ChR2}-LHb (72.20 ± 5.798 s vs. 131.9 ± 9.382 s, t = 5.136, p = 0.0006). (**q**) Time spent in the center zone of the open field during optogenetic activation of LHA^{mCh}-LHb and LHA^{ChR2}-LHb (12.70 ± 0.8678 s vs. 23.60 ± 1.438 s, t = 6.152, p = 0.0002). (**r**) Number of line crossings in the open field during optogenetic activation of LHA^{mCh}-LHb and LHA^{ChR2}-LHb (49.80 ± 4.420 vs. 104.5 ± 9.451, t = 4.891, p = 0.0009). Data are presented as the mean ± SEM. *p < 0.05, **p < 0.01 (unpaired t-test). LHA, lateral hypothalamic area; LHb, lateral habenula.

social stress (Arendt et al., 2014), and stimulation of OxR2 by intra-cerebroventricular infusion of a modified orexin B peptide enhances resilience to social stressors (Staton et al., 2018), suggesting an anxiolytic and antidepressant effect of OxR2 activation. However, some clinical studies have reported contradictory results of OxR2. Seltorexant (JNJ-42847922/MIN-202), an OxR2 antagonist, was reported to induce antidepressant effects in clinical patients (Brooks et al., 2019; Recourt et al., 2019). It is noteworthy that patients enrolled in these clinical trials with MDD were likely to be very different from animal models of CSDS in terms of brain states and mechanisms. Due to the influence of the orexinergic systems on sleep-wake regulation, the sleep-consolidation effect of seltorexant may greatly contribute to the improvement of depressive symptoms of these patients. In addition, oral administration of seltorexant in clinical trials with its systematic influence would not be comparable with our circuit-specific manipulation. Our study emphasizes the specificity of OxR2 in the LHb in mediating the anxiolytic and antidepressant effects after chronic social stress. Both our study (Supplementary Fig. 4) and previous reports showed that OxR2 has a larger population in the LHb than OxR1 (Hashikawa et al., 2020; Zhang et al., 2018), indicating that OxR2 is more likely involved in the modulation of LHb function. However, the regulatory effect of OxR1 signaling in the LHb is worth investigating in the future.

In comparison with the recent study by Flanigan et al. in which the orexinergic projections to the LHb encoded the aggressive behavior of the resident mice during social interaction with weak intruder mice (Flanigan et al., 2020), we focused on the role of orexinergic projections to the LHb in the socially defeated intruder. Although we used the same model of social stress, we assessed the distinct behaviors of mice with different social characteristics. In their study, optogenetic activation of orexin inputs to the LHb enhanced aggressive behaviors and aggression-conditioned place preference, suggesting the rewarding properties of this circuit. Our study demonstrated that infusion of orexin A or activation of orexinergic terminals in the LHb reduced the immobility time in both the TST and FST, indicating the antidepressnt properties of this circuit. In addition, both aggression and anti-depression are self-protective in response to stress. Therefore, it is not surprising, but rather is interesting to observe a similar protective characteristic of LHb orexinergic innervations in the socially aggressive mice and socially defeated mice. However, Flanigan et al. revealed a microcircuit in which orexin could exert feedforward inhibition to LHb glutamatergic neurons by activating LHb GAD2-positive neurons through OxR2 signaling. In contrast, our study emphasized the direct effect of orexinergic neurons on glutamatergic neurons in the LHb. Hence, the distinction and interaction between these two parallel circuits requires further investigation.

The current study has several limitations. Although we did not find a significant increase in LHb GAD2 neuron excitability in defeated mice, GAD2 neurons are still a potential target for orexinergic regulation in the socially defeated state (Flanigan et al., 2020). Moreover, we identified the activation of glutamatergic and OxR2-expressing neurons in the LHb after social defeat stress, and LHA orexinergic projections to the LHb are involved in CSDS-induced maladaptive behaviors. However, direct innervation from LHA orexinergic neurons to the LHb glutamatergic neurons still lacks anatomical evidence. Moreover, it has been reported that orexin exhibits dimorphic alterations between male and female subjects in both clinical and animal studies (Grafe, Cornfeld, et al., 2017; Lu et al., 2017; Mikrouli et al., 2011), yet the social defeat model in the present study consisted only male mice, which might not represent the integrated function of orexin in both sexes.

5. Conclusion

In summary, we identified the anxiolytic and antidepressant effects of the circuit from LHA orexinergic neurons to the LHb in response to chronic social stress. Our findings provide new evidence of the antidepressant properties of LHA orexin circuits and support the orexinergic systems as a potential target for the development of novel therapeutics for stress-related disorders.

Data availability

Data will be made available on request

CRediT authorship contribution statement

Dan Wang: Investigation, Data curation, Methodology, Visualization. **Ao Li:** Data curation, Visualization, Writing - original draft. **Keyi Dong:** Investigation, Writing - original draft. **Huihui Li:** Investigation. **Yongxin Guo:** Investigation. **Xinxin Zhang:** Software. **Min Cai:** Writing - review & editing. **Huiming Li:** Writing - review & editing. **Guangchao Zhao:** Writing - review & editing, Funding acquisition. **Qianzi Yang:** Conceptualization, Supervision, Validation, Funding acquisition.

Declaration of competing interest

The authors have no competing interests to declare.

Appendix A. Supplementary data

Supplementary data to this article can be found online at https://doi.org/10.1016/j.ynstr.2021.100298.

References

Allen, W.E., DeNardo, L.A., Chen, M.Z., Liu, C.D., Loh, K.M., Fenno, L.E., Ramakrishnan, C., Deisseroth, K., Luo, L., 2017. Thirst-associated preoptic neurons encode an aversive motivational drive. Science 357, 1149–1155. https://doi.org/10.1126/science.aan6747.

Ammoun, S., Holmqvist, T., Shariatmadari, R., Oonk, H.B., Detheux, M., Parmentier, M., Akerman, K.E., Kukkonen, J.P., 2003. Distinct recognition of OX1 and OX2 receptors by orexin peptides. J. Pharmacol. Exp. Therapeut. 305, 507–514. https://doi.org/10.1124/jpet.102.048025.

Arendt, D.H., Hassell, J., Li, H., Achua, J.K., Guarnieri, D.J., Dileone, R.J., Ronan, P.J., Summers, C.H., 2014. Anxiolytic function of the orexin 2/hypocretin A receptor in the basolateral amygdala. Psychoneuroendocrinology 40, 17–26. https://doi.org/10.1016/j.psyneuen.2013.10.010.

Arendt, D.H., Ronan, P.J., Oliver, K.D., Callahan, L.B., Summers, T.R., Summers, C.H., 2013. Depressive behavior and activation of the orexin/hypocretin system. Behav. Neurosci. 127, 86–94. https://doi.org/10.1037/a0031442.

Barthas, F., Hu, M.Y., Siniscalchi, M.J., Ali, F., Mineur, Y.S., Picciotto, M.R., Kwan, A.C., 2020 Oct 1. Cumulative effects of social stress on reward-guided actions and prefrontal cortical activity. Biol. Psychiatr. 88 (7), 541–553. https://doi.org/10.1016/j.biopsych.2020.02.008. Epub 2020 Feb 19.

Blouin, A.M., Fried, I., Wilson, C.L., Staba, R.J., Behnke, E.J., Lam, H.A., Maidment, N.T., Karlsson, K.Æ., Lapierre, J.L., Siegel, J.M., 2013. Human hypocretin and melanin-concentrating hormone levels are linked to emotion and social interaction. Nat. Commun. 4 https://doi.org/10.1038/ncomms2461.

Broberger, C., De Lecea, L., Sutcliffe, J.G., Hokfelt, T., 1998. Hypocretin/orexin- and melanin-concentrating hormone-expressing cells form distinct populations in the rodent lateral hypothalamus: relationship to the neuropeptide Y and agouti gene-related protein systems. J. Comp. Neurol. 402, 460–474.

Brooks, S., Jacobs, G.E., de Boer, P., Kent, J.M., Van Nueten, L., van Amerongen, G., Zuiker, R., Kezic, I., Luthringer, R., van der Ark, P., van Gerven, J.M., Drevets, W., 2019. The selective orexin-2 receptor antagonist seltorexant improves sleep: an exploratory double-blind, placebo controlled, crossover study in antidepressant-

treated major depressive disorder patients with persistent insomnia. J. Psychopharmacol. 33, 202–209. https://doi.org/10.1177/0269881118822258.

Brundin, L., Björkqvist, M., Petersén, A., Träskman-Bendz, L., 2007a. Reduced orexin levels in the cerebrospinal fluid of suicidal patients with major depressive disorder. Eur. Neuropsychopharmacol 17, 573–579. https://doi.org/10.1016/j.euroneuro.2007.01.005.

Brundin, L., Petersén, A., Björkqvist, M., Träskman-Bendz, L., 2007b. Orexin and psychiatric symptoms in suicide attempters. J. Affect. Disord. 100, 259–263. https://doi.org/10.1016/j.jad.2006.10.019.

Cengiz, M., Karaj, V., Kocabasoglu, N., Gozubatik-Celik, G., Dirican, A., Bayoglu, B., 2019. Orexin/hypocretin receptor, Orx1, gene variants are associated with major depressive disorder. Int. J. Psychiatr. Clin. Pract. 23, 114–121. https://doi.org/10.1080/13651501.2018.1551549.

Chang, H., Saito, T., Ohiwa, N., Tateoka, M., Deocaris, C.C., Fujikawa, T., Soya, H., 2007. Inhibitory effects of an orexin-2 receptor antagonist on orexin A- and stress-induced ACTH responses in conscious rats. Neurosci. Res. 57, 462–466. https://doi.org/10.1016/j.neures.2006.11.009.

Chung, H.S., Kim, J.G., Kim, J.W., Kim, H.W., Yoon, B.J., 2014. Orexin administration to mice that underwent chronic stress produces bimodal effects on emotion-related behaviors. Regul. Pept. 194–195, 16–22. https://doi.org/10.1016/j.regpep.2014.11.003.

Cohen, S., Matar, M.A., Vainer, E., Zohar, J., Kaplan, Z., Cohen, H., 2020. Significance of the orexinergic system in modulating stress-related responses in an animal model of post-traumatic stress disorder. Transl. Psychiatry 10, 10. https://doi.org/10.1038/s41398-020-0698-9.

Cui, Y., Yang, Y., Ni, Z., Dong, Y., Cai, G., Foncelle, A., Ma, S., Sang, K., Tang, S., Li, Y., Shen, Y., Berry, H., Wu, S., Hu, H., 2018. Astroglial Kir4.1 in the lateral habenula drives neuronal bursts in depression. Nature 554, 323–327. https://doi.org/10.1038/nature25752.

De Boer, P., Drevets, W.C., Rofael, H., van der Ark, P., Kent, J.M., Kezic, I., Parapatics, S., Dorffner, G., van Gerven, J., Benes, H., Keicher, C., Jahn, H., Seiden, D.J., Luthringer, R., 2018. A randomized Phase 2 study to evaluate the orexin-2 receptor antagonist seltorexant in individuals with insomnia without psychiatric comorbidity. J. Psychopharmacol. 32, 668–677. https://doi.org/10.1177/0269881118773745.

Eacret, D., Grafe, L.A., Dobkin, J., Gotter, A.L., Renger, J.J., Winrow, C.J., Bhatnagar, S., 2019. Orexin signaling during social defeat stress influences subsequent social interaction behaviour and recognition memory. Behav. Brain Res. 356, 444–452. https://doi.org/10.1016/j.bbr.2018.05.032.

Flanigan, M.E., Aleyasin, H., Li, L., Burnett, C.J., Chan, K.L., LeClair, K.B., Lucas, E.K., Matikainen-Ankney, B., Durand-de Cuttoli, R., Takahashi, A., Menard, C., Pfau, M.L., Golden, S.A., Bouchard, S., Calipari, E.S., Nestler, E.J., DiLeone, R.J., Yamanaka, A., Huntley, G.W., Clem, R.L., Russo, S.J., 2020. Orexin signaling in GABAergic lateral habenula neurons modulates aggressive behavior in male mice. Nat. Neurosci. 23, 638–650. https://doi.org/10.1038/s41593-020-0617-7.

Giardino, W.J., Eban-Rothschild, A., Christoffel, D.J., Li, S.B., Malenka, R.C., de Lecea, L., 2018. Parallel circuits from the bed nuclei of stria terminalis to the lateral hypothalamus drive opposing emotional states. Nat. Neurosci. 21, 1084–1095. https://doi.org/10.1038/s41593-018-0198-x.

Golden, S.A., Covington 3rd, H.E., Berton, O., Russo, S.J., 2011. A standardized protocol for repeated social defeat stress in mice. Nat. Protoc. 6, 1183–1191. https://doi.org/10.1038/nprot.2011.361.

Gonzalez, J.A., Iordanidou, P., Strom, M., Adamantidis, A., Burdakov, D., 2016. Awake dynamics and brain-wide direct inputs of hypothalamic MCH and orexin networks. Nat. Commun. 7, 11395. https://doi.org/10.1038/ncomms11395.

Grafe, L.A., Bhatnagar, S., 2018. Orexins and stress. Front. Neuroendocrinol. 51, 132–145. https://doi.org/10.1016/j.yfrne.2018.06.003.

Grafe, L.A., Cornfeld, A., Luz, S., Valentino, R., Bhatnagar, S., 2017a. Orexins mediate sex differences in the stress response and in cognitive flexibility. Biol. Psychiatr. 81, 683–692. https://doi.org/10.1016/j.biopsych.2016.10.013.

Grafe, L.A., Eacret, D., Dobkin, J., Bhatnagar, S., 2018. Reduced orexin system function contributes to resilience to repeated social stress. eNeuro 5. https://doi.org/10.1523/ENEURO.0273-17.2018.

Grafe, L.A., Eacret, D., Luz, S., Gotter, A.L., Renger, J.J., Winrow, C.J., Bhatnagar, S., 2017b. Orexin 2 receptor regulation of the hypothalamic-pituitary-adrenal (HPA) response to acute and repeated stress. Neuroscience 348, 313–323. https://doi.org/10.1016/j.neuroscience.2017.02.038.

Hashikawa, Y., Hashikawa, K., Rossi, M.A., Basiri, M.L., Liu, Y., Johnston, N.L., Ahmad, O.R., Stuber, G.D., 2020. Transcriptional and spatial resolution of cell types in the mammalian habenula. Neuron 106, 743–758. https://doi.org/10.1016/j.neuron.2020.03.011 e745.

Hu, H., Cui, Y., Yang, Y., 2020. Circuits and functions of the lateral habenula in health and in disease. Nat. Rev. Neurosci. 21, 277–295. https://doi.org/10.1038/s41583-020-0292-4.

Huang, L., Xi, Y., Peng, Y., Yang, Y., Huang, X., Fu, Y., Tao, Q., Xiao, J., Yuan, T., An, K., Zhao, H., Pu, M., Xu, F., Xue, T., Luo, M., So, K.F., Ren, C., 2019. A visual circuit related to habenula underlies the antidepressive effects of light therapy. Neuron 102, 128–142. https://doi.org/10.1016/j.neuron.2019.01.037 e128.

Ito, N., Yabe, T., Gamo, Y., Nagai, T., Oikawa, T., Yamada, H., Hanawa, T., 2008. I.c.v. administration of orexin-A induces an antidepressive-like effect through hippocampal cell proliferation. Neuroscience 157, 720–732. https://doi.org/10.1016/j.neuroscience.2008.09.042.

Jalewa, J., Wong-Lin, K., McGinnity, T.M., Prasad, G., Holscher, C., 2014. Increased number of orexin/hypocretin neurons with high and prolonged external stress-induced depression. Behav. Brain Res. 272, 196–204. https://doi.org/10.1016/j.bbr.2014.05.030.

James, M.H., Campbell, E.J., Dayas, C.V., 2017. Role of the orexin/hypocretin system in stress-related psychiatric disorders. In: Behavioral Neuroscience of Orexin/Hypocretin, pp. 197–219.

Ji, M.J., Zhang, X.Y., Chen, Z., Wang, J.J., Zhu, J.N., 2019. Orexin prevents depressive-like behavior by promoting stress resilience. Mol. Psychiatr. 24, 282–293. https://doi.org/10.1038/s41380-018-0127-0.

Kendler, K.S., Karkowski, L.M., Prescott, C.A., 1999. Causal relationship between stressful life events and the onset of major depression. Am. J. Psychiatr. 156, 837–841. https://doi.org/10.1176/ajp.156.6.837.

Khairuddin, S., Aquili, L., Heng, B.C., Hoo, T.L.C., Wong, K.H., Lim, L.W., 2020. Dysregulation of the orexinergic system: a potential neuropeptide target in depression. Neurosci. Biobehav. Rev. 118, 384–396. https://doi.org/10.1016/j.neubiorev.2020.07.040.

Kim, T.-K., Kim, J.-E., Park, J.-Y., Lee, J.-E., Choi, J., Kim, H., Lee, E.-H., Kim, S.-W., Lee, J.-K., Kang, H.-S., Han, P.-L., 2015. Antidepressant effects of exercise are produced via suppression of hypocretin/orexin and melanin-concentrating hormone in the basolateral amygdala. Neurobiol. Dis. 79, 59–69. https://doi.org/10.1016/j.nbd.2015.04.004.

Kudryavtseva, N.N., Smagin, D.A., Kovalenko, I.L., Vishnivetskaya, G.B., 2014. Repeated positive fighting experience in male inbred mice. Nat. Protoc. 9, 2705–2717. https://doi.org/10.1038/nprot.2014.156.

Li, J., Li, H., Wang, D., Guo, Y., Zhang, X., Ran, M., Yang, C., Yang, Q., Dong, H., 2019. Orexin activated emergence from isoflurane anaesthesia involves excitation of ventral tegmental area dopaminergic neurones in rats. Br. J. Anaesth. 123, 497–505. https://doi.org/10.1016/j.bja.2019.07.005.

Lu, J., Zhao, J., Balesar, R., Fronczek, R., Zhu, Q.B., Wu, X.Y., Hu, S.H., Bao, A.M., Swaab, D.F., 2017. Sexually dimorphic changes of hypocretin (orexin) in depression. EBioMedicine 18, 311–319. https://doi.org/10.1016/j.ebiom.2017.03.043.

Lutter, M., Krishnan, V., Russo, S.J., Jung, S., McClung, C.A., Nestler, E.J., 2008. Orexin signaling mediates the antidepressant-like effect of calorie restriction. J. Neurosci. 28, 3071–3075. https://doi.org/10.1523/JNEUROSCI.5584-07.2008.

McEwen, B.S., 2007. Physiology and neurobiology of stress and adaptation: central role of the brain. Physiol. Rev. 87, 873–904. https://doi.org/10.1152/physrev.00041.2006.

Mikrouli, E., Wortwein, G., Soylu, R., Mathe, A.A., Petersen, A., 2011. Increased numbers of orexin/hypocretin neurons in a genetic rat depression model. Neuropeptides 45, 401–406. https://doi.org/10.1016/j.npep.2011.07.010.

Monteleone, A.M., Ruzzi, V., Patriciello, G., Cascino, G., Pellegrino, F., Vece, A., Monteleone, P., Maj, M., 2020. Emotional reactivity and eating disorder related attitudes in response to the trier social stress test: an experimental study in people with anorexia nervosa and with bulimia nervosa. J. Affect. Disord. 274, 23–30. https://doi.org/10.1016/j.jad.2020.05.051.

Nambu, T., Sakurai, T., Mizukami, K., Hosoya, Y., Yanagisawa, M., Goto, K., 1999. Distribution of orexin neurons in the adult rat brain. Brain Res. 827, 243–260. https://doi.org/10.1016/s0006-8993(99)01336-0.

Nocjar, C., Zhang, J., Feng, P., Panksepp, J., 2012. The social defeat animal model of depression shows diminished levels of orexin in mesocortical regions of the dopamine system, and of dynorphin and orexin in the hypothalamus. Neuroscience 218, 138–153. https://doi.org/10.1016/j.neuroscience.2012.05.033.

Nollet, M., Gaillard, P., Minier, F., Tanti, A., Belzung, C., Leman, S., 2011. Activation of orexin neurons in dorsomedial/perifornical hypothalamus and antidepressant reversal in a rodent model of depression. Neuropharmacology 61, 336–346. https://doi.org/10.1016/j.neuropharm.2011.04.022.

Pan, Y.P., Liu, C., Liu, M.F., Wang, Y., Bian, K., Xue, Y., Chen, L., 2020. Involvement of orexin-A in the regulation of neuronal activity and emotional behaviors in central amygdala in rats. Neuropeptides 80, 102019. https://doi.org/10.1016/j.npep.2020.102019.

Rainero, I., Ostacoli, L., Rubino, E., Gallone, S., Picci, L.R., Fenoglio, P., Negro, E., Rosso, C., De Martino, P., De Marchi, M., Furlan, P.M., Pinessi, L., 2011. Association between major mood disorders and the hypocretin receptor 1 gene. J. Affect. Disord. 130, 487–491. https://doi.org/10.1016/j.jad.2010.10.033.

Razzoli, M., Pearson, C., Crow, S., Bartolomucci, A., 2017. Stress, overeating, and obesity: insights from human studies and preclinical models. Neurosci. Biobehav. Rev. 76, 154–162. https://doi.org/10.1016/j.neubiorev.2017.01.026.

Recourt, K., de Boer, P., Zuiker, R., Luthringer, R., Kent, J., van der Ark, P., Van Hove, I., van Gerven, J., Jacobs, G., van Nueten, L., Drevets, W., 2019. The selective orexin-2 antagonist seltorexant (JNJ-42847922/MIN-202) shows antidepressant and sleep-promoting effects in patients with major depressive disorder. Transl. Psychiatry 9, 216. https://doi.org/10.1038/s41398-019-0553-z.

Ren, S., Wang, Y., Yue, F., Cheng, X., Dang, R., Qiao, Q., Sun, X., Li, X., Jiang, Q., Yao, J., Qin, H., Wang, G., Liao, X., Gao, D., Xia, J., Zhang, J., Hu, B., Yan, J., Wang, Y., Xu, M., Han, Y., Tang, X., Chen, X., He, C., Hu, Z., 2018. The paraventricular thalamus is a critical thalamic area for wakefulness. Science 362, 429–434. https://doi.org/10.1126/science.aat2512.

Sakurai, T., 2014. The role of orexin in motivated behaviours. Nat. Rev. Neurosci. 15, 719–731. https://doi.org/10.1038/nrn3837.

Scott, M.M., Marcus, J.N., Pettersen, A., Birnbaum, S.G., Mochizuki, T., Scammell, T.E., Nestler, E.J., Elmquist, J.K., Lutter, M., 2011. Hcrtr1 and 2 signaling differentially regulates depression-like behaviors. Behav. Brain Res. 222, 289–294. https://doi.org/10.1016/j.bbr.2011.02.044.

Shang, C., Liu, A., Li, D., Xie, Z., Chen, Z., Huang, M., Li, Y., Wang, Y., Shen, W.L., Cao, P., 2019. A subcortical excitatory circuit for sensory-triggered predatory hunting in mice. Nat. Neurosci. 22, 909–920. https://doi.org/10.1038/s41593-019-0405-4.

Staton, C.D., Yaeger, J.D.W., Khalid, D., Haroun, F., Fernandez, B.S., Fernandez, J.S., Summers, B.K., Summers, T.R., Sathyanesan, M., Newton, S.S., Summers, C.H., 2018.

Orexin 2 receptor stimulation enhances resilience, while orexin 2 inhibition promotes susceptibility, to social stress, anxiety and depression. Neuropharmacology 143, 79–94. https://doi.org/10.1016/j.neuropharm.2018.09.016.

Steru, L., Chermat, R., Thierry, B., Simon, P., 1985. The tail suspension test: a new method for screening antidepressants in mice. Psychopharmacology (Berl) 85, 367–370. https://doi.org/10.1007/bf00428203.

Summers, C.H., Yaeger, J.D.W., Staton, C.D., Arendt, D.H., Summers, T.R., 2020. Orexin/hypocretin receptor modulation of anxiolytic and antidepressive responses during social stress and decision-making: potential for therapy. Brain Res. 1731, 146085. https://doi.org/10.1016/j.brainres.2018.12.036.

Van Someren, E.J.W., 2020 Aug 13. Brain mechanisms of insomnia: new perspectives on causes and consequences. Physiol. Rev. https://doi.org/10.1152/physrev.00046.2019. Online ahead of print.

Wang, D., Li, Y., Feng, Q., Guo, Q., Zhou, J., Luo, M., 2017. Learning shapes the aversion and reward responses of lateral habenula neurons. Elife 6. https://doi.org/10.7554/eLife.23045.

Yang, Y., Cui, Y., Sang, K., Dong, Y., Ni, Z., Ma, S., Hu, H., 2018. Ketamine blocks bursting in the lateral habenula to rapidly relieve depression. Nature 554, 317–322. https://doi.org/10.1038/nature25509.

Zhang, L., Hernandez, V.S., Swinny, J.D., Verma, A.K., Giesecke, T., Emery, A.C., Mutig, K., Garcia-Segura, L.M., Eiden, L.E., 2018. A GABAergic cell type in the lateral habenula links hypothalamic homeostatic and midbrain motivation circuits with sex steroid signaling. Transl. Psychiatry 8, 50. https://doi.org/10.1038/s41398-018-0099-5.